PHILOSOPHICAL TRANSACTIONS OF THE ROYAL SOCIETY A MATHEMATICAL, PHYSICAL & ENGINEERING SCIENCES

Time and frequency resolved ZEKE spectra and the interseries dynamics of high molecular Rydberg states

F. Remacle

Phil. Trans. R. Soc. Lond. A 1997 **355**, 1701-1705
doi: 10.1098/rsta.1997.0086

Time and frequency resolved ZEKE spectra and the interseries dynamics of high molecular Rydberg states

By F. Remacle†

Département de Chimie, B6, Université de Liège, B 4000 Liège, Belgium

ZEKE spectroscopy is based on delayed detection by pulsed field ionization. At a given excitation frequency, the time evolution of the Rydberg states that survive can be monitored from sub μs to tens of μs delay times. We compute time and frequency resolved ZEKE spectra (Remacle *et al.* 1996) for a realistic molecular Hamiltonian including the effect of a weak external DC field. The decay kinetics obtained from the full dynamical computations can be accurately represented by two time scales (μs and supra μs) as reported experimentally. The long lifetimes are accounted for by the extensive interseries coupling induced by the anisotropy of the molecular core.

1. Physical aspects of ZEKE spectra

ZEKE spectra differ from ordinary photoionization spectra in that only states that have not yet ionized (or predissociated) after a finite time delay are detected. Not all nearly isoenergetic states are detected: the states detected are those that can be pulsed field ionized for a given field strength and fall within the detection window. The depth of this window depends on the threshold for ionization and, at a given excitation energy, is different for different series. By varying the depth of the detection window, one can therefore harvest different Rydberg series. One important aspect of ZEKE spectroscopy is that an appropriate detection scheme provides a resolution of the individual thresholds since each state of the ionic core is characterized by its own ZEKE peak. The reason is that the states excited at frequencies not immediately below the threshold decay faster. Therefore, while the overall peak intensity decreases with time, there is a more pronounced early time decrease on the red side of the peak.

The formalism (Remacle *et al.* 1996) that we use to compute time- and frequency-resolved ZEKE spectra follows the sequence of experimental steps: (i) the molecule is excited for a long interval taken to be from $-\infty$ to time $t = 0$; (ii) at time $t = 0$, the laser is turned off and the system evolves under its own Hamiltonian plus the external perturbations that are present in the experiment; (iii) at time t, $t > 0$, the detection, that counts all the states within the detection window, is applied. This formalism captures the essential features of the experimentally observed spectra, as can be seen from the time dependent line shape plotted in figure 1. The computations are for a one series model where the time evolution is mimicked by assigning to each bound state a width of Γ_0/n^3, where n is the principal quantum number of the Rydberg

† Chercheur Qualifié, FNRS, Belgium.

Phil. Trans. R. Soc. Lond. A (1997) **355**, 1701–1705
Printed in Great Britain

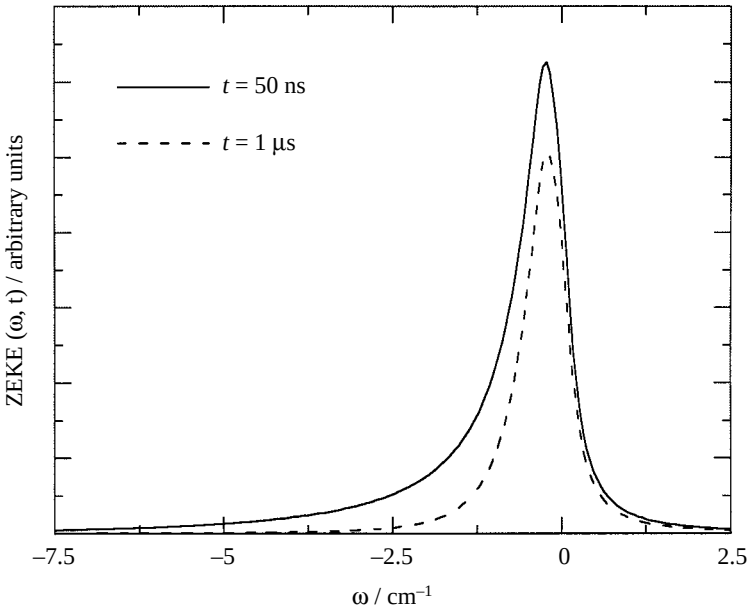

Figure 1. Time-dependent line shape for delay times of 50 ns and 1 μs before detection. The laser width is $0.2\,\mathrm{cm}^{-1}$ and Γ_0 is equal to $100\,\mathrm{cm}^{-1}$. Note that the spectrum can also be inhomogeneously broaden by a thermal distribution of initial states.

state. There is a ZEKE peak hugging the threshold because while the line shape of each state is spread, its maximum is reduced by n^3/Γ_0 in order to preserve a unit area. The overall spectra exhibit the characteristic asymmetric shape, with a faster loss of population on the red side. If $\Gamma_0 \to 0$, the computation recovers the expected flat spectrum since the optical transition to bound high Rydberg states scales as n^{-3} and in a given series, there are n^3 states per energy interval. At lower n, the spectrum exhibits individual features which can be resolved by the laser.

2. Computational results

Multiseries computations are carried out for realistic molecular parameters of Na_2^+ in the presence of a weak external DC field using an effective Hamiltonian formalism (Remacle & Levine 1996). The zero-order basis is an inverse Born–Oppenheimer picture where each vibrotational state of the ionic core carries its own Rydberg series. The anisotropy of the molecular core induces interseries coupling between the different Rydberg series and therefore leads to a break down of the Born–Oppenheimer limit. We compute the interseries matrix elements exactly (Remacle & Levine 1996; Baranov *et al.* 1996). Above the first threshold for ionization, the core-electron interaction is responsible for the coupling between bound states isoenergetic with the continua, leading to the autoionization process. The interseries coupling is also effective between quasi isoenergetic bound states belonging to different Rydberg series. Above the Inglis–Teller (I–T) limit, interseries mixing is assisted by the stray field which makes the density of states in both series more uniform. States above the detection threshold in a given series can disappear by exiting the detection window due to the coupling to a higher j series (j is the rotational quantum number of the core). Therefore, ZEKE spectra evolve with time in a possibly non-monotonic way.

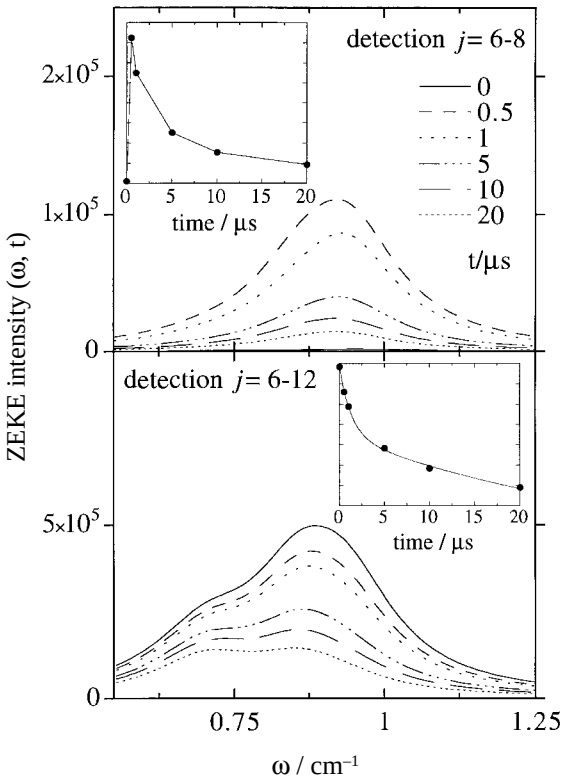

Figure 2. Computed ZEKE spectra versus laser frequency ω, where $\omega = 0$ is the lowest threshold for ionization, for a laser width of 0.2 cm^{-1} and different delays before the ionization. Four series corresponding to zero-order states: $j = 6$, $n = 168$–176; $j = 8$, $n = 124$–127; $j = 10$, $n = 98$–100; $j = 12$, $n = 82$, with $l = 0, 1, \ldots, n-1$ for each n value are retained in the computations. $M = 0$. The frequency range is centred at 0.9 cm^{-1} between the (lowered by the external field) ionization thresholds of $j = 4$ and $j = 6$.

Interseries coupling is also responsible for the fact that states that have not been optically excited (e.g. due to Franck Condon factors or rotational selection rules) can be detected. Computed spectra for increasing delays before ionization and two kinds of detection windows (see Remacle *et al.* (1996) and Remacle & Levine (1996) for more details) are plotted in figure 2 for a basis set including four Rydberg series ($j = 6$, 8, 10 and 12) coupled by the quadrupolar term of the core-electron interaction in the presence of a weak external DC field of 0.1 V cm^{-1}. The optical excitation is into the $l \leqslant 2$ states of the $j = 10$ and 12 series. Similar plots have been obtained for a lower strength ($F_s = 0.01$ V cm^{-1}) of the stray field. The detection window in the upper panel is limited to the $j = 6$ and 8 series. At very short times, there is somewhat less signal because there is no direct optical excitation in these series. However, while the laser is on (for $t < 0$), some zero-order population is shifted in these series by the interseries coupling, so that by $t = 0$, a low but finite intensity is already detectable. Then, the population in the bound series reaches a steady state and the overall ZEKE intensity decreases with time. Without the interseries coupling induced by the core, there would not be any ZEKE signal in the upper panel of figure 2. Note also that the intensity (in arbitrary units) is about five times larger for the spectrum shown in the lower panel where the initially excited series are included in the detection window.

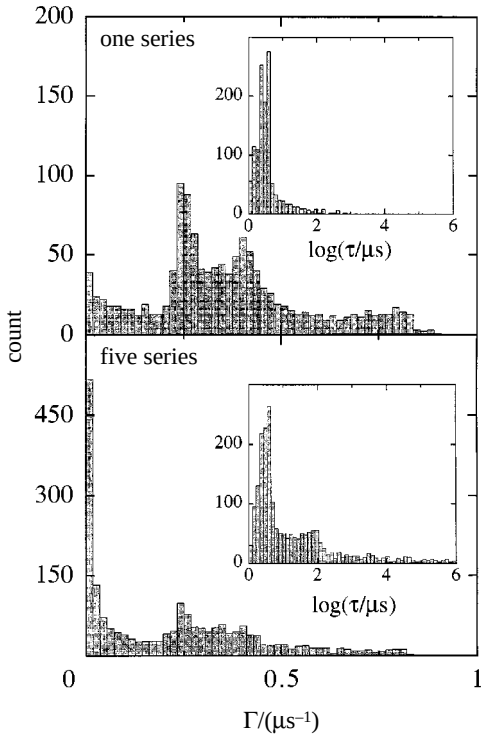

Figure 3. Histograms of the individual decay widths (plotted versus width in μs^{-1} on a linear scale) for a $j = 4$ single series (upper panel) and a $j = 4, 6, 8, 10$ and 12 five series (lower panel) computation for the molecular parameters of Na_2^+ in the presence of a stray external DC field of 0.01 V cm^{-1}, $M = 0$. The retained quasi-isoenergetic zero states are $j = 4$, $n = 248$–252 for the one series computation and $j = 4$, $n = 248$–252; $j = 6$, $n = 161$–163; $j = 8$, $n = 121$; $j = 10$, $n = 97$; $j = 12$, $n = 81$ for the five series histogram. All Rydberg states $l = 0, 1, \ldots, n-1$ are included in both basis sets. The inserts show the plot of the lifetimes (in μs) on a logarithmic scale to emphasize the bimodal character of the distribution and the separation of time scales. Note that there are many more larger widths (= shorter decay times) in the one series computation.

For each spectrum, the insert shows the decay of the integrated ZEKE intensity versus time (in μs). The decay kinetics is found to very accurately exhibit two time scales, just as has been observed. The fit to a biexponential form is extremely tight ($\rho_{corr} > 0.999$) and the short and the long decay times are 1.3 and 30 μs, respectively. The two time scales of the decay kinetics are related to the bimodal character of the distribution of the individual lifetimes and to the dynamical bottlenecks identified in phase space (Remacle & Levine 1996). The latter are due to an incomplete mixing of zero-order states, which is typical of highly dense structures that are coupled to a smaller number of decay channels. Three bottlenecks, responsible for the stability of Rydberg states, are identified: (i) first bottleneck: incomplete l mixing; (ii) second bottleneck: incomplete j mixing; (iii) third bottleneck: no M mixing. In the absence of perturbation by neighbouring ions and/or an external magnetic field, the projection quantum number $M = m_l + m_j$ is conserved. For higher values of M, the bound series exhibits an extreme stability (Remacle & Levine 1996). Histograms of the individual lifetimes obtained by numerical diagonalization of the effective Hamiltonian are plotted in figure 3 for one series ($j = 4$) and five series ($j = 4$, 6, 8, 10, 12) computations in Na_2^+ in the presence of a weak external DC field of 0.01 V cm^{-1}.

The series that is directly coupled to an ionization continuum is the same for both computations ($j = 4$). l-mixing, which is the only mechanism operative in the one series computation, is not sufficient to account for the long lifetimes. They are essentially due to the second bottleneck and incomplete interseries mixing between the Rydberg series that is directly coupled to the ionization continuum and those which are not.

The long time component observed in the decay kinetics (inserts of figure 2) is significant (up to 40%) and does not require the effect of external ions (which is not included in the present computation). In our computations which are above the lowest IP, efficient interseries coupling is sufficient to account for the long decay times of tens of μs (figure 3 lower panel). When we include predissociation, the intensity of the long time component is reduced but still significant. We expect that the presence of ions will enhance the extent of the long time decay and increase its decay constant. In particular below the lowest IP, where autoionization is not possible, external perturbations can play a bigger role in the time evolution of the optically excited state.

This work has been carried out with Professor R. D. Levine, at the Hebrew University of Jerusalem. The computational work was supported by SFB 377. I thank Professor U. Even, Professor E. W. Schlag, Dr L. Ya Baranov and Dr E. Rabani for many discussions.

References

Baranov, L. Y., Remacle, F. & Levine, R. D. 1996 *Phys. Rev.* A **54**, 4789.

Remacle, F. & Levine, R. D. 1996 *J. Chem. Phys.* **105**, 4649.

Remacle, F., Even, U. & Levine, R. D. 1996 *J. Phys. Chem.* **100**, 19 735.

PHILOSOPHICAL TRANSACTIONS OF THE ROYAL SOCIETY A MATHEMATICAL, PHYSICAL & ENGINEERING SCIENCES